Dual Function FH MIMO Radar System with DPSK Signal Embedding

Indu Priya Eedara and Moeness G. Amin

Centre for Advanced Communications, Villanova University, Villanova, PA, 19085, USA
E-mail: {ieedara; moeness.amin}@villanova.edu

***Abstract*—In this paper, we propose a method for information embedding into the emission of frequency hopping (FH) multiple-input multiple-output (MIMO) radar. The differential phase shift keying (DPSK) modulated communication symbols are embedded into each pulse of the FH radar waveforms. We examine the effect of DPSK symbol embedding on the radar operation by analyzing the range sidelobes performance, power spectral density (PSD) and data rate of the system. The proposed system shows significant reduction in range sidelobes, good spectral containment and achieves high communication data rates. The latter is enabled by synthesizing a large number of orthogonal waveforms.**

I. Introduction

Co-existence between radar and communications has been proposed as a solution to the spectral congestion caused by the increasing demands from the wireless industry in [1]–[3]. When communications is treated as secondary to the primary radar function, the system is referred to as dual-function radar-communication (DFRC) [4], [5]. DFRC systems make full use of the radar resources such as high quality hardware and high transmit power. For the DFRC system, information embedding into the emission of single-input multiple-output (SIMO) radar can be achieved using waveform diversity, sidelobe control, or time modulated array [6]. Information embedding into the emission of multiple-input multiple-output (MIMO) radar was considered in [7]–[10]. Alternative names used in the literature for the DFRC system are Intentional Modulation on a Pulse and CoRadar [11], [12].

In this paper, we embed the communication symbols in the radar pulses in fast time. Specifically, we propose a waveform design where we embed differential phase shift keying (DPSK) symbols into the frequency hopping (FH) pulses. FH waveforms have constant modulus and are simple to generate [13]. Modulating the FH waveforms by phase shift keying (PSK) symbols, presented in [8], disrupts the continuous phase of the FH waveforms between the sub-pulses, and hence results in undesirable spectral leakage [14]. In order to maintain the phase continuity between the sub-pulses, we propose the use of DPSK signalling which assumes better spectral containment compared to that of PSK scheme. Each symbol is represented by a unique sequence of phases implemented using DPSK. In essence, the FH pulses, transmitted over each pulse repetition interval and from each antenna, are modulated by DPSK waveforms. The nominal FH-based MIMO radar without any communication embedding, can exhibit high range sidelobes due to the re-use of FH coefficients within the same pulse [15]. We demonstrate that the randomness underlying the DPSK causes significant reduction in the range sidelobes of the FH MIMO radar system, and as a result, a large number of orthogonal FH waveforms can be synthesized by allowing increased rate of FH coefficient recurrence.

One embedding approach to preserve the continuous phase between the FH sub-pulses uses different combinations of FH sequences to represent the communication bits [16]. However, this system suffers from high range sidelobes due to the re-use of the FH coefficients in the single pulse duration. Also, owing to the use of unique combinations of frequencies to define communication symbols, the number of waveforms that can be synthesized to achieve high data rate becomes limited. With the proposed DPSK embedding, we can achieve low range sidelobes, good spectral containment and high communication data rates that come about from the ability of synthesizing a large number of orthogonal waveforms.

The paper is organized as follows. The details of the DFRC system design, the FH waveforms, DPSK symbol embedding, bandwidth requirements and the MIMO radar receive signal models are presented in Sec.II. Analysis of the FH/DPSK waveform design is presented in Sec. III, and the conclusions are drawn in Sec IV.

II. MIMO radar Signal Model

We consider a system equipped with a common dual-function transmit platform. The common transmit array comprises M omni-directional co-located transmit antennas and the MIMO radar receive array has N antennas arranged in a linear shape. For MIMO system, the radar transmit waveforms $\phi_m(t)$, $m = 1 \dots M$, should satisfy the orthogonality condition, i.e.,

$$\int_{T_p} \phi_m(t)\phi^*_{m'}(t+\tau)e^{j2\pi\nu t}dt = \begin{cases} \delta(\tau)\delta(\nu), & m = m', \\ 0, & \text{otherwise} \end{cases} \quad (1)$$

where, t is the fast-time index, T_p is the pulse duration, $(\cdot)^*$ denotes the conjugate of a complex number, τ and ν denote time delay and the Doppler shift, respectively and $\delta(\cdot)$ is the Kronecker delta function. It is difficult to synthesize waveforms which satisfy the ideal orthogonality condition (1).

This work is supported by NSF award #AST- 1547420.

978-9-0827-9703-9/19/$31.00 ©2019 IEEE

Practical waveforms, which can be efficiently synthesized, are discussed in [9] and references therein.

A. Frequency-Hopping Waveforms

FH waveforms are inherently power efficient due to the constant-modulus property. They are also simple to generate and have low probability of intercept (LPI). Further, FH waveforms meet the MIMO radar requirements, such as high transmit power efficiency, high range and Doppler resolution properties. These properties have motivated the use of FH waveforms for MIMO radar [13], [17]. The FH waveform from m^{th} antenna can be expressed as,

$$\phi_m(t) = \sum_{q=1}^{Q} e^{j2\pi c_{m,q}\Delta_f t} u(t - q\Delta_t), \tag{2}$$

where $c_{m,q},\ m = 1, \ldots, M,\ q = 1, \ldots, Q$ denote the FH coefficients, Q is the number of sub-pulses derived from K available frequencies ($K \geq Q$), Δ_f and Δ_t are the frequency step and the sub-pulse duration, respectively, and

$$u(t) \triangleq \begin{cases} 1, & 0 < t < \Delta_t, \\ 0, & \text{otherwise.} \end{cases} \tag{3}$$

is a rectangular pulse of duration Δ_t. Equation (2) implies that each FH waveform contains Q sub-pulses, i.e., the radar pulse duration $T_p = Q\Delta_t$. It is also assumed that $\Delta_t\Delta_f$ is an integer. In this paper, we choose $\Delta_t\Delta_f = 1$. Selection of FH code matrix, whose elements are $c_{m,q}$, is important for designing the FH waveforms and was investigated in [13].

B. DPSK signalling scheme

Use of continuous phase shift modulation (CPSM) to modulate radar pulses, leading to improved performance, was discussed in [18]. In CPSM, due to the continuous phase across bit boundaries, the spectral spreading is low compared to other phase modulation methods, such as PSK. DPSK, minimum shift keying (MSK), and continuous phase modulation (CPM) are types of modulations considered under the auspices of CPSM. Since the first derivative of the phase for MSK and CPM modulations is continuous, these signals have better spectral containment compared to that of the DPSK modulation [19], [20]. On the otherhand, DPSK exhibits better range sidelobe structure. Therefore, we limit our discussion of FH sub-pulses with DPSK phase modulated waveforms, and implement the signal structure presented in [21]. For high power applications, radar codes must be constant modulus so as to maximize the energy on the target. Therefore, codes are typically designed with the implicit assumption that each code value is modulated onto a square-shaped chip. Since there are Q sub-pulses available in the FH radar pulse, each information symbol is described by a sequence of Q code phase values, represented by square shaped pulses of width Δ_t. These phase values Ω_q^b, are drawn from the constellation defined by $\Omega_q^b \in \mathbb{D} = \left\{0, \frac{2\pi}{J}, \ldots, \frac{(J-1)2\pi}{J}\right\}$, where J is the constellation size. The information symbol can be represented by a sequence of Q phases as,

$$s_b(t) = \sum_{q=1}^{Q} e^{j\Omega_q^b} \left[u(t - (q-1)\Delta_t) - u(t - q\Delta_t)\right], \tag{4}$$

where, Ω_q^b is the phase value of the q^{th} sub-pulse corresponding to the information symbol b, and $u(t)$ is the unit step function. The total number of combinations of the information sequences $(s_b(t))$ achieved from this configuration is J^Q. The DPSK modulation of the code sequence in (4) is given by,

$$\psi_b(t) = s_b\left(t - \Delta_t/2\right)\left|\cos\left(\frac{\pi t}{\Delta_t}\right)\right| - j s_b(t)\left|\sin\left(\frac{\pi t}{\Delta_t}\right)\right|, \tag{5}$$

where, the code values are contained in $s_b(t)$ from (4). The above equation infers that the phase of $\psi_b(t)$ is continuous across the sub-pulse boundaries $q\Delta_t$. For the sake of simplicity, and for all practical purposes, we assume $J = 2$, i.e., $\Omega_q^b \in (0, \pi)$. Therefore, the total number of waveforms that can be designed from the underlying configuration is 2^Q.

C. Proposed DFRC waveforms

Below, we propose a method of modulating the FH MIMO radar waveforms defined in (2) by symbols selected from the dictionary constructed in (5). The FH MIMO radar waveform modulated by DPSK communication symbols in fast-time is shown in Fig. 1. Here, each FH radar pulse from each

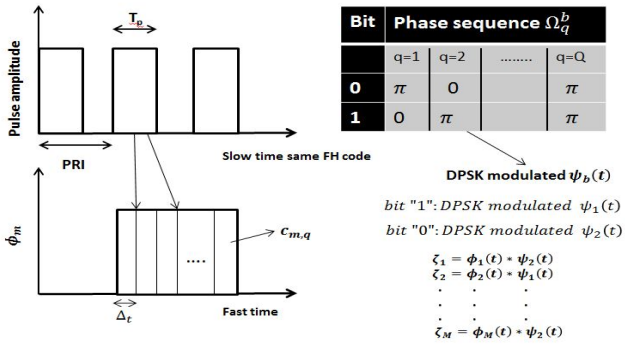

Fig. 1: Proposed scheme of modulation.

antenna is embedded with one communication symbol which is represented by Q phase code values. The DPSK modulated FH waveform from m^{th} antenna can be expressed as,

$$\zeta_m(t) = \phi_m(t).\psi_b(t). \tag{6}$$

From (6), if the size of the dictionary, $\psi_b(t) = 2$, i.e., $\psi_b(t) = \{\psi_1(t), \psi_2(t)\}$, one bit of information is embedded in $\zeta_m(t)$. In this case, either bit $'1'$ or bit $'0'$ is transmitted from each antenna depending on the DPSK waveform selected. If $\psi_b(t) = \{\psi_1(t), \psi_2(t), \psi_3(t), \psi_4(t)\}$, one of the bit sequences $\{00, 01, 10, 11\}$, i.e., 2 bits of information is transmitted from each antenna. Also, in FH DFRC, an additional constraint on

the orthogonality between the FH waveforms from one sub-pulse to another across antennas is mandated by the communication function of the system. In essence, the condition,

$$c_{m,q} \neq c_{m',q}, \qquad \forall q, m \neq, m' \tag{7}$$

should be satisfied in the FH code matrix to enable symbol detection at the communication receiver.

D. Bandwidth Requirements

Let B denote the bandwidth assigned to the DFRC system. To insure that the spectral contents of the orthogonal FH waveforms are confined to the available bandwidth, the FH code, $c_{m,q}$ should be selected from the set of integers $\{0, 1, \ldots, K-1\}$, where $K \approx \frac{B}{\Delta_f}$,

$$B_{\text{eff}} \approx (K-1)\Delta_f + \frac{1}{\Delta_t}, \tag{8}$$

and the condition $B_{\text{eff}} \leq B$ is satisfied. The time-bandwidth product of the DFRC system is given as,

$$BT_p = \left((K-1)\Delta_f + \frac{1}{\Delta_t}\right) Q\Delta_t = KQ. \tag{9}$$

E. MIMO Radar Receive Signal Model

Assume that the signals reflected by L targets impinge on the MIMO radar receiver from directions $\theta_\ell,\ \ell = 1, \ldots, L$. The $N \times\ 1$ complex-valued vector of the received baseband signals can be represented as,

$$\mathbf{x}(t,n) = \sum_{\ell=1}^{L} \beta_\ell(n) \left[\mathbf{a}^T(\theta_\ell)\, \boldsymbol{\zeta}(t,n)\right] \mathbf{b}(\theta_\ell) + \mathbf{z}(t,n), \tag{10}$$

where n denotes the slow-time index, i.e., pulse number, $\beta_\ell(n)$ is the reflection coefficient associated with the ℓ^{th} target during the n^{th} pulse, θ_ℓ is the spatial angle of the ℓ^{th} target, $\mathbf{a}(\theta_\ell)$ and $\mathbf{b}(\theta_\ell)$ are the steering vectors of the transmit and receive arrays towards direction θ_ℓ, respectively, $(\cdot)^T$ stands for the transpose, $\boldsymbol{\zeta}(t,n) \triangleq [\zeta_1(t,n), \ldots, \zeta_M(t,n)]^T$ is the $M \times\ 1$ complex vector of DPSK modulated waveforms, and $\mathbf{z}(t,n)$ is an $N \times 1$ vector of zero-mean white Gaussian noise with variance σ_z^2. Matched filtering (10) to the transmitted orthogonal waveforms yields the $MN \times 1$ data vector

$$\begin{aligned}\mathbf{y}(n) &= \text{vec}\left(\int_{T_p} \mathbf{x}(t,n)\, \boldsymbol{\zeta}(t,n)^H(t)\, dt\right) \\ &= \sum_{\ell=1}^{L} \beta_\ell(n) \left[\mathbf{a}(\theta_\ell) \otimes \mathbf{b}(\theta_\ell)\right] + \tilde{\mathbf{z}}(n),\end{aligned} \tag{11}$$

where $\text{vec}(\cdot)$ denotes the vectorization operator that stacks the columns of a matrix into one long column vector, $\otimes$ denotes the Kronecker product, $(\cdot)^H$ stands for the Hermitian transpose, $\tilde{\mathbf{z}}(n)$ is $MN \times 1$ vector of additive noise at the output of the matched-filters with zero-mean and co-variance $\sigma_z^2 \mathbf{I}_{MN}$, and $\mathbf{I}_M$ is the identity matrix of size $M \times M$.

Consider a single-antenna communication receiver located at in the spatial direction θ_c with respect to the MIMO radar. The signal at the output of the communication receiver is

$$r(t,n) = \alpha_{\text{ch}} \mathbf{a}^T(\theta_c) \boldsymbol{\zeta}(t,n) + w(t,n), \tag{12}$$

where α_{ch} is the channel coefficient which summarizes the propagation environment between the transmit array and the communication receiver and $w(t,n)$ represents the additive white Gaussian noise with zero mean and variance σ_w^2.

Assume that time and phase synchronizations between the MIMO radar and the communication receiver are achieved. Then, matched filtering $r(t,n)$ to the FH sub-pulses yields

$$\begin{aligned}y_{m,q}(n) &= \int_{\Delta_t} r(t,n) h_{m,q}^*(t) u(t - q\Delta_t - nT_0) dt \\ &= \alpha_{\text{ch}} e^{j\left(\Omega_{p,m}^{(n)} - 2\pi d_m \sin\theta_c\right)} + w_{m,q}(n),\end{aligned} \tag{13}$$

where, $h_{m,q}(t) \triangleq e^{j2\pi c_{m,q}\Delta_f t}$ is the FH signal associated with the m^{th} antenna during the q^{th} sub-pulse, d_m is the displacement between the first and the m^{th} elements of the transmit array measured in wavelength, and $w_{m,q}(n) \triangleq \int_0^{\Delta_t} w(t,n) e^{-j2\pi c_{m,q}\Delta_f t} u(t - \Delta_t - nT_0) dt$ is the additive noise term at the output of the $(m,q)^{\text{th}}$ matched filter with zero mean and variance σ_w^2. Then, the embedded DPSK symbols are demodulated.

III. Analysis of the proposed DFRC waveforms

In this section, we analyze the range sidelobes performance, power spectral density and the communication data rate that can be achieved by the proposed configuration of the waveforms.

A. Range sidelobe performance

1) Without DPSK Embedding: Without loss of generality, we consider the case of a DFRC system with uniform linear arrays. The inter-element spacings associated with the transmit and receive arrays are denoted as d_T and d_R, respectively. The spatial frequency of a target located in direction θ is defined as $f = 2\pi d_R sin(\theta)$, where d_R is measured in wavelength. Adopting the AF definition from [17], the AF expression for the MIMO radar can be written as,

$$|\chi(\tau,\nu,f,f')| \triangleq \left|\sum_{m=1}^{M}\sum_{m'=1}^{M} \chi_{m,m'}(\tau,\nu) e^{j2\pi(fm - f'm')\gamma}\right|, \tag{14}$$

where, τ, ν, f, f' denote time delay, Doppler shift, spatial frequency, and spatial frequency shift, respectively, and $\gamma \triangleq d_T/d_R$. For zero Doppler shift ($\nu = 0$) and $f = f'$, we can compute the range sidelobe response from (14) for FH MIMO radar waveforms as,

$$\Gamma_{\text{rad}}(\tau) = \chi_{m,m'}(\tau,0) \triangleq \int_0^{T_p} \phi_m(t) \phi_{m'}^*(t+\tau), \tag{15}$$

where, $\Gamma_{\text{rad}}(\tau)$ is the correlation function between the FH waveforms from antennas m and m'. At delays $\tau = i\Delta_t$, $i = 0, 1, \ldots, Q-1$, due to the re-use of frequencies in the FH sub-pulses, the FH MIMO radar system exhibits high range sidelobes [15].

2) With DPSK Embedding: The range sidelobe levels for the DFRC system with DPSK symbol embedding can be computed as,

$$\Gamma_{\mathrm{DF}}(\tau) = \chi_{m,m'}(\tau, 0) \triangleq \int_0^{T_p} \zeta_m(t)\zeta^*_{m'}(t+\tau). \qquad (16)$$

At $\tau = i\Delta_t$, due to the randomness of the DPSK phase values, the terms inside the summations of (14) cancel each other, resulting in significant reduction of the range sidelobe levels. As a result, a large number of DFRC waveforms can be synthesized with frequency re-use among the sub-pulses. When all the antennas transmit the same communication symbol, the proposed system shows significant reduction in the range sidelobes, unlike the DFRC system in [15]. This is due to the fact that each communication symbol is phase coded in the proposed waveform modulation.

As an example, we consider the values of $M = K = Q = 16$, when there is maximum re-use of frequencies. One bit of information per antenna is selected and transmitted from a sequence of $[1011101010101011]$ bits, during one pulse duration. Bits 1 and 0 are represented by a unique sequence of Q phase code values drawn from $[0, \pi]$, and this sequence is modulated using DPSK. The range sidelobe response for such sequence is presented in Fig. 2a, where it is evident that the DPSK symbol embedding yields significant reduction of the range sidelobes. We also, present a worst case scenario where all antennas transmit the same information symbol, i.e., all antennas transmit waveform embedded with information bit $'1'$. From Fig. 2b, it can be clearly observed that the randomness in the phase values result in low range sidelobes even for the same symbol embedding. A 3D plot of the ambiguity function (AF) is shown in Fig. 3 to demonstrate the effect of DPSK symbol embedding along both delay and the Doppler axes. It is shown that the reduction is more significant along the delay axis compared to the Doppler axis.

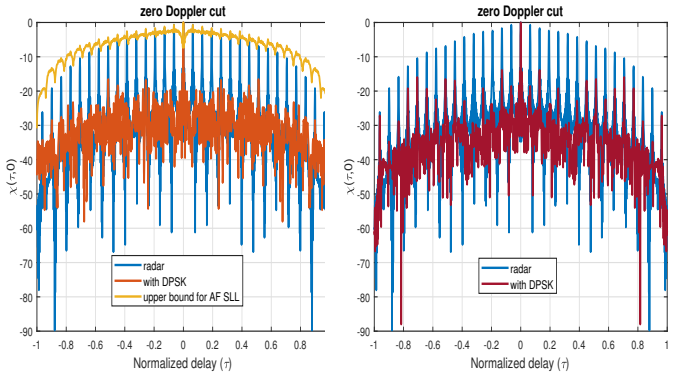

(a) With and without DPSK information embedding (b) Worst case scenario

Fig. 2: Zero Doppler cuts showing the effect of DPSK symbol embedding on the FH MIMO radar system.

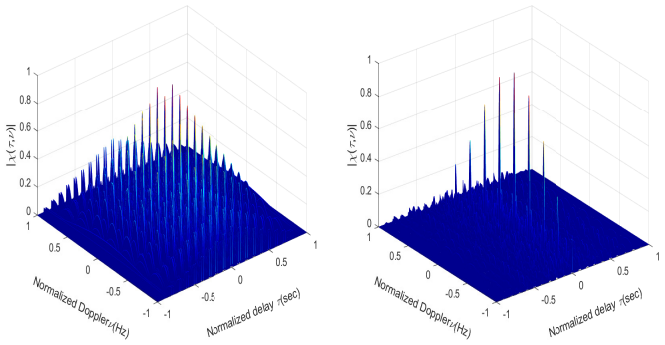

(a) AF before embedding (b) AF after symbol embedding

Fig. 3: AF plots before and after DPSK symbol embedding.

B. Power Spectral Density (PSD)

The effect of DPSK symbol embedding on the PSD of the FH MIMO system is presented in this sub-section. Unlike PSK symbol embedding, the DPSK modulation presented in this paper results in smooth transitions between the FH MIMO sub-pulses. Therefore the DPSK symbol embedding leads to lower spectral sidelobes compared to that of the PSK embedding. Since the first derivative of the phase for the DPSK modulation is not continuous, this can still cause spectral broadening [18]. This can be avoided by setting few of the phase values used to define the symbols at the high and low frequencies of the spectrum, $\Omega_q^b = 0°$. From Fig. 4, it is evident that the spectral sidelobes of the DFRC system with DPSK embedding are lower compared to that of the DFRC system with PSK embedding.

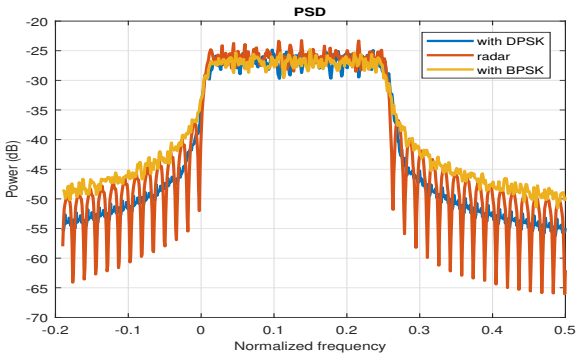

Fig. 4: PSD of the FH MIMO radar system with and without symbol embedding.

C. Data Rate

In this sub-section, we present the data rate that can be achieved by this proposed configuration.

Each FH MIMO radar pulse from each antenna has Q sub-pulses and hence, each communication symbol can be represented by Q phase values. Therefore, the total number of symbols that can be represented by this configuration is J^Q. The maximum number of bits of information that can be transmitted are $Q.log_2 J$. For the proposed DFRC MIMO system,

the data rate that can be achieved is $DR = M.Q.log_2 J.PRF$. As the DPSK constellation increases, the data rate of the system increases. When $K = 20$, the maximum bit rate achieved by the proposed system for DPSK configuration with $J = 2$, $M = 20$ and $Q = 20$ is 40 Mbps. This is higher than the maximum bit rate that can achieved by the modulation technique through FH code selection in [16], which is 34 Mbps for $M = 10$ and $Q = 20$. Also, there is a two fold increase in the number of orthogonal waveforms that can be synthesized by the proposed modulation compared to that of [16].

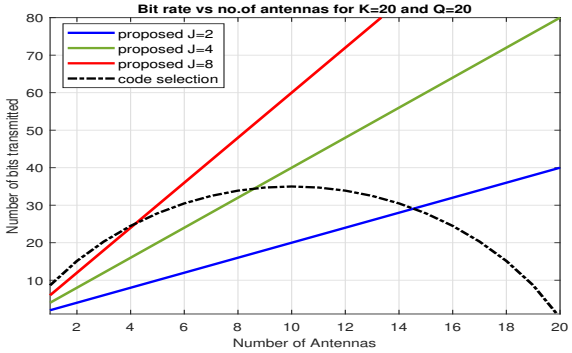

Fig. 5: Achievable bit rates for the proposed scheme.

For the proposed modulation, it is evident from Fig. 5 that, the bit rate increases with the number of antennas and the size of the phase constellation. The modulation proposed through FH code selection in [16] achieves maximum bit rate for $M = K/2$. But, for $M > K/2$, the bit rate decreases with increased number of antennas. This, in turn, limits the data rate of the system and also, the number of orthogonal waveforms that can be synthesized. With our proposed modulation, high data rates can be achieved by increasing the size of phase constellation and by synthesizing large number of orthogonal waveforms.

IV. Conclusion

In this paper, we proposed the modulation of FH MIMO radar waveforms in fast time by DPSK information symbols. We analyzed the effect of DPSK symbol embedding on the FH MIMO radar system functionality by examining the range sidelobes performance, the power spectral density and the data rate achieved by the system. Due to the randomness of the phase values used to represent the communication symbols, the DPSK embedding showed a significant reduction in the range sidelobes. The proposed modulation also preserves the continuous phase between the FH sub-pulses and hence spectral sidelobes are lower compared to those associated with PSK symbol embedding. The high data rate under the proposed configuration was also derived.

References

[1] H. Griffiths, S. Blunt, L. Cohen, and L. Savy, "Challenge problems in spectrum engineering and waveform diversity," in *Proc. IEEE Radar Conf.*, April 2013, pp. 1–5.

[2] C. Baylis, M. Fellows, L. Cohen, and R. J. M. II, "Solving the spectrum crisis: Intelligent, reconfigurable microwave transmitter amplifiers for cognitive radar," *IEEE Microwave Magazine*, vol. 15, no. 5, pp. 94–107, July 2014.

[3] P. M. McCormick, S. D. Blunt, and J. G. Metcalf, "Simultaneous radar and communications emissions from a common aperture, part I: Theory," in *Proc. IEEE Radar Conf.*, May 2017, pp. 1685–1690.

[4] A. Hassanien, M. G. Amin, Y. D. Zhang, and F. Ahmad, "Dual-function radar-communications: Information embedding using sidelobe control and waveform diversity," *IEEE Transactions on Signal Processing*, vol. 64, no. 8, pp. 2168–2181, April 2016.

[5] A. Hassanien, M. G. Amin, Y. D. Zhang, and F. Ahmad, "Signaling strategies for dual-function radar communications: an overview," *IEEE Aerospace and Electronic Systems Magazine*, vol. 31, no. 10, pp. 36–45, October 2016.

[6] J. Euzire, R. Guinvarc'h, M. Lesturgie, B. Uguen, and R. Gillard, "Dual function radar communication Time-modulated array," in *2014 International Radar Conference*, Oct 2014, pp. 1–4.

[7] B. Li and A. Petropulu, "MIMO radar and communication spectrum sharing with clutter mitigation," in *2016 IEEE Radar Conference (RadarConf)*, May 2016, pp. 1–6.

[8] A. Hassanien, B. Himed, and B. D. Rigling, "A dual-function MIMO radar-communications system using frequency-hopping waveforms," in *Proc. IEEE Radar Conf.*, May 2017, pp. 1721–1725.

[9] S. D. Blunt and E. L. Mokole, "Overview of radar waveform diversity," *IEEE Aerospace and Electronic Systems Magazine*, vol. 31, no. 11, pp. 2–42, November 2016.

[10] S. Amuru, R. M. Buehrer, R. Tandon, and S. Sodagari, "MIMO radar waveform design to support Spectrum Sharing," in *MILCOM 2013 - 2013 IEEE Military Communications Conference*, Nov 2013, pp. 1535–1540.

[11] M. J. Nowak, Z. Zhang, Y. Qu, D. A. Dessources, M. Wicks, and Z. Wu, "Co-designed radar-communication using linear frequency modulation waveform," in *MILCOM 2016 - 2016 IEEE Military Communications Conference*, Nov 2016, pp. 918–923.

[12] D. Gaglione, C. Clemente, C. V. Ilioudis, A. R. Persico, I. K. Proudler, J. J. Soraghan, and A. Farina, ""waveform design for communicating radar systems using fractional Fourier transform"," *Digital Signal Processing*, vol. 80, pp. 57 – 69, 2018. [Online]. Available: http://www.sciencedirect.com/science/article/pii/S1051200418302070

[13] K. Han and A. Nehorai, "Jointly optimal design for MIMO radar frequency-hopping waveforms using game theory," *IEEE Transactions on Aerospace and Electronic Systems*, vol. 52, no. 2, pp. 809–820, April 2016.

[14] I. P. Eedara, M. G. Amin, and A. Hassanien, "Analysis of communication symbol embedding in FH MIMO radar platforms," in *Proc. IEEE Radar Conf*, April 2019.

[15] I. P. Eedara, A. Hassanien, M. G. Amin, and B. D. Rigling, "Ambiguity Function analysis for dual-function radar communications using PSK signaling," in *2018 52nd Asilomar Conference on Signals, Systems, and Computers*, Oct 2018, pp. 900–904.

[16] W. Baxter, E. Aboutanios, and A. Hassanien, "Dual-function MIMO radar-communications via frequency-hopping code selection," in *2018 52nd Asilomar Conference on Signals, Systems, and Computers*, Oct 2018, pp. 1126–1130.

[17] C. Y. Chen and P. P. Vaidyanathan, "MIMO radar ambiguity properties and optimization using frequency-hopping waveforms," *IEEE Transactions on Signal Processing*, vol. 56, no. 12, pp. 5926–5936, Dec 2008.

[18] H. H. Faust, B. Connolly, T. M. Firestone, R. C. Chen, B. H. Cantrell, and E. L. Mokole, "A spectrally clean transmitting system for solid-state phased-array radars," in *Proceedings of the 2004 IEEE Radar Conference (IEEE Cat. No.04CH37509)*, April 2004, pp. 140–144.

[19] S. Blunt, M. Cook, E. Perrins, and J. de Graaf, "Cpm-based radar waveforms for efficiently bandlimiting a transmitted spectrum," in *2009 IEEE Radar Conference*, May 2009, pp. 1–6.

[20] I. P. Eedara and M. G. Amin, "Performance trade-off analysis of co-design of radar and phase modulated communication signals in frequency hopping MIMO systems," 05 2019, p. 19.

[21] S. D. Blunt, M. R. Cook, and J. Stiles, "Embedding information into radar emissions via waveform implementation," in *2010 International Waveform Diversity and Design Conference*, Aug 2010, pp. 000 195–000 199.